Proceedings of the ASME/ASCE/IEEE 2011 Joint Rail Conference
JRC2011
March 16-18, 2011, Pueblo, Colorado, USA

JRC2011-56064

APPLICATION OF NADAL LIMIT IN THE PREDICTION OF WHEEL CLIMB DERAILMENT

Brian Marquis
U.S. Department of Transportation
Research and Innovative Technology Administration
Volpe National Transportation Systems Center
Cambridge, Massachusetts, United States

Robert Greif[1]
U.S. Department of Transportation
Research and Innovative Technology Administration
Volpe National Transportation Systems Center
Cambridge, Massachusetts, United States

ABSTRACT

Application of the Nadal Limit to the prediction of wheel climb derailment is presented along with the effect of pertinent geometric and material parameters. Conditions which contribute to this climb include wheelset angle of attack, contact angle, friction and saturation surface properties, and lateral and vertical wheel loads. The Nadal limit is accurate for high angle of attack conditions, as the wheelset rolls forward in quasi-static steady motion leading to a flange climbing scenario. A detailed study is made of the effect of flange contact forces F_{tan} and N, the tangential friction force due to creep and the normal force, respectively. Both of these forces vary as a function of lateral load L. It is shown that until a critical value of L/V is reached, climb does not occur with increasing L since Ftan is saturated and the flange contact point slides down the rail. However, for a certain critical value of L/V (i.e. the Nadal limit) F_{tan} is about to drop below its saturated value and flange climb (rolling without sliding) up the rail occurs. Additionally, an alternative explanation of climb is given based on a comparison of force resultants in track and contact coordinates.

The effects of longitudinal creep force F_{long} and angle of attack are also investigated. Using a saturated creep resultant based on both (F_{tan}, F_{long}) produces a climb prediction L/V larger (less conservative) than the Nadal limit. Additionally, for smaller angle of attack the standard Nadal assumption of $F_{tan}=\mu N$ may lead to an overly conservative prediction for the onset of wheel climb. Finally, a useful analogy for investigating conditions for sliding and/or rolling of a wheelset is given from a study of a disk in rigid body mechanics.

INTRODUCTION

The Federal Railroad Administration (FRA) has studied and evaluated derailments of railcars for many years in order to ensure the safety of the railroad fleet. One derailment mode of particular interest involves conditions under which a flanging wheel can climb (roll without sliding) up on a rail and in the extreme case can roll onto the top of the railhead. There are many conditions which can contribute to this wheel climb including wheel angle of attack, contact angle, friction and saturation surface properties, and lateral and vertical wheel load. One of the first studies of this phenomenon was done by Nadal [1] who related flanging wheel force in track coordinates to equivalent forces in contact coordinates. This produces a relationship between L, V the lateral and vertical wheel loads in track coordinates, and the forces in the flange contact plane F_{tan}, N the tangential friction force due to creep and the normal force, respectively. This relationship leads to the Nadal limit for the prediction of the onset of wheel climb. The difficulty of completely understanding wheel climb is illustrated by the large number of papers that have been written on this subject through the years including Gilchrist and Brickle [2], Weinstock [3], Elkins and Shust [4],[5] and Blader [6],[7]. It should be noted that the Nadal limit is accurate for high angle of attack (AOA) conditions associated with $F_{tan} > F_{long}$, as the wheelset rolls forward in quasi-static steady motion leading to a flange climbing scenario. Dynamic transient effects, including impacts, pulses and other short duration effects, might require higher L/V and a different physical mechanism for derailment to occur. However, even for these dynamic transient conditions the FRA continues to apply the Nadal limit because it is a conservative derailment indicator. The Nadal limit is used as a safety criterion in FRA's existing and

[1] Professor Emeritus, Department of Mechanical Engineering, Tufts University, Medford, MA.

proposed [8] high-speed track safety standards (speeds exceeding 90 mph) to minimize the risk of wheel climb derailment. The formula referenced in these FRA standards assumes a coefficient of friction of 0.5 (to establish a conservative limit) and requires that the L/V during testing shall not exceed the limit for more than 5 feet. FRA believes this criterion also provides some protection against other concerns, rather than just wheel climb, including overloading track components and equipment component failures.

A detailed study is made of F_{tan} and N, both of which vary as a function of lateral load L. In steady-state curving it is typical to have the flanging wheel of the wheelset moving along the rail with tread contact and a second point of contact on the flange. With L and hence L/V relatively low, derailment does not occur and the flange contact point slides down the rail with a saturated value of F_{tan}. As L increases, there is a certain value of L at which F_{tan} is about to drop *below* its saturated value. At this point the flange contact condition will change from sliding down the rail which preserves wheelset forward motion, to a *climbing* (rolling without sliding) upward on the rail as the wheelset travels along the rail. This point for the onset of wheel climb is shown to be precisely the Nadal limit, and L/V can then be written in terms of the friction coefficient μ between the flanging wheel and the rail, and also δ the flange contact angle. This paper also introduces an alternative way of explaining the onset of wheelset climb based on Nadal theory from a comparison of the flanging wheel force resultant in track coordinates with the force resultant in the contact plane. The onset of wheel climb occurs when the force resultants are exactly equal in both magnitude and direction.

A useful analogy for understanding these concepts are the conditions for the sliding (spinning) and/or rolling of a disk in rigid body mechanics. An example is shown relating disk forces and disk geometry subject to a friction constraint, to the ensuing dynamic rolling motion of the disk. Two further wheelset effects are studied for their impact on wheel climb conditions – namely the effect of longitudinal creep and also the effect of wheelset angle of attack. The relation of longitudinal creep force F_{long} and also wheelset angle of attack to the onset of wheel climb is discussed. The resultant friction force in the contact plane can be constructed from the F_{tan} and F_{long} components. When the resultant saturates at μN, its lateral component F_{tan} is reduced below μN leading to a generalized L/V expression which is larger (less conservative) than the Nadal Limit in predicting the onset of wheel climb. The second effect, namely angle of attack ψ, is important since F_{tan} in steady state curving is directly proportional to ψ (neglecting spin creep effects). When the resultant friction force saturates while ψ is smaller, F_{tan} is reduced while F_{long} is increased causing the Nadal limit based on $F_{tan} = \mu \cdot N$ to predict a smaller critical L/V (perhaps significantly smaller) for the prediction of the onset of wheel climb, which may lead to an overly conservative result.

WHEEL RAIL INTERACTION AND FORCES

Consider Figure 1 in which the lead flanging wheel is at the outer rail and is set at a positive angle of attack. L and V represent the lateral and vertical forces acting on the rail in track coordinates while F_{tan} and N in contact coordinates represent the reacting wheel friction force due to creep and normal force, respectively. The angle δ is the contact angle between the wheel flange and the rail in track coordinates. It is useful to consider both sets of forces (L, V and F_{tan}, N) acting either on the rail or the wheel. In Figure 2 both sets of forces are shown acting on the wheel, each set having the common resultant force R.

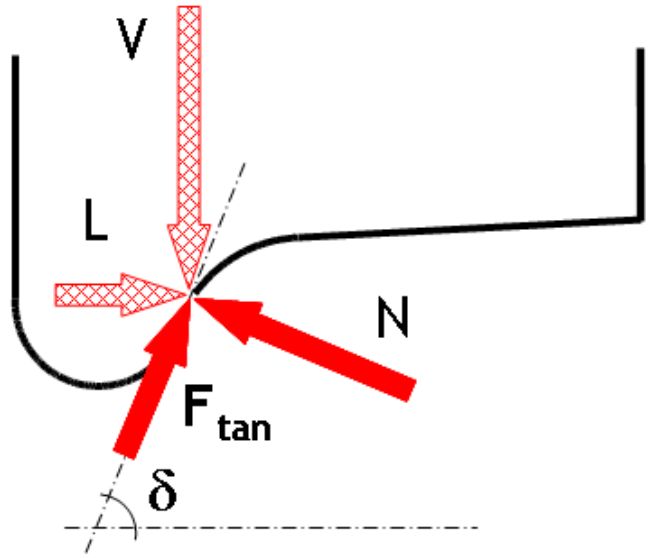

Figure 1 Forces on rail (L,V) and wheel (F_{tan}, N)

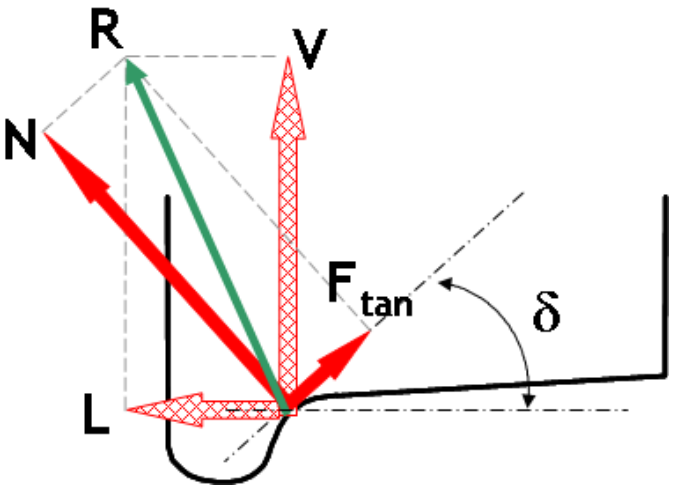

Figure 2 Forces on wheel (track and contact coordinates)

The equivalence among these sets of forces in Figure 2 may be considered by a simple coordinate transformation:

$$L = -F_{tan} \cdot \cos\delta + N \cdot \sin\delta, \quad V = F_{tan} \cdot \sin\delta + N \cdot \cos\delta \qquad (1)$$

Solving these equations produces the relation:

$$L/V = (\tan\delta - F_{tan}/N)/(1 + (F_{tan}/N) \cdot \tan\delta) \qquad (2)$$

In equation (2), assuming the friction force F_{tan} is saturated at a maximum value of $\mu \cdot N$, where μ is the coefficient of friction, leads to a minimum value of L/V and the Nadal limit:

$$L/V = (\tan\delta - \mu)/(1 + \mu \cdot \tan\delta) \qquad (3)$$

Based on field work and test data it has been shown that this Nadal limit is a conservative lower bound in the prediction of the onset of wheel climb. Nadal, in his derivation for incipient climb, had assumed that the flanging wheel was in single point contact involving the wheel flange. For these same conditions used in the current paper of a high positive angle of attack with quasi –static steady motion, we may assume that *initially t*here is two point contact involving the wheel tread and flange, with the flange contact point located ahead of the tread contact point as shown in Figure 3. As the wheelset travels with its forward motion, the flange contact point is continuously sliding down the rail and the friction force $F_{tan} = \mu \cdot N$ is saturated. Wheel climb occurs in the limit when the flange friction force drops *below* its saturated value of μN and the wheel then starts to climb (roll without sliding) up the rail along the flange in a single point contact condition. The Nadal limit equation (3) is

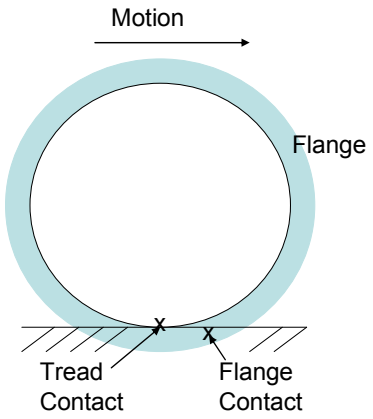

Figure 3 Two point contact for positive AOA of wheel to rail - contact point on flange leading contact point on tread

obtained from equation (2) as a minimum L/V associated with the maximum friction value of $F_{tan} = \mu \cdot N$. It is important to note that that for the high AOA quasi-static steady rolling conditions the *direction* of the friction force F_{tan} remains the same as shown in Figure 2 whether the wheel is climbing up the rail on the flange or the flange contact force is sliding down relative to the rail.

The flange contact force has a tangential component and also a longitudinal friction force F_{long} due to longitudinal creep. The effect of this longitudinal component is to consume part of the maximum available friction force in the lateral plane depicted by Figure 2, so that F_{tan} would not be able to reach the full limiting value of $\mu \cdot N$. Then application of equation (2) would produce a larger (less conservative) value for the limiting L/V for predicting wheel climb than that of the Nadal Limit of equation (3). An engineering approach to the inclusion of longitudinal friction effects on the prediction of wheel climb is included later on in this paper.

CLIMBING AND SLIDING CHARACTERISTICS

The interaction between the saturation of the friction force and wheel climbing/sliding characteristics can be explained in detail using Figures 4 and 5. Figure 4 explains this interaction involving lateral force L, while Figure 5 explains this interaction using a wheel force vector diagram in which L,V are in track coordinates and N, F_{tan} are in contact coordinates. Since the lateral force acting on a wheelset is a key driving force in the mechanics of a wheel climb derailment, results are plotted against L/V (with V held constant) in Figure 4 and interpreted as a function of lateral force variation. The results for this motion shown in Figure 4 with quasi-static, steady, and high-positive AOA can also explain why, depending on the value of lateral force, for the same value of contact friction force the wheel may climb up or it may experience sliding down on its flange. Using the parameter values of friction coefficient $\mu = 0.5$, vertical wheel load V = 12,500 pounds and flange angle $\delta = 60$ degrees, values of F_{tan} and N can be found as a function of lateral force L from equation (1). Note that L and N are linearly proportional so that an increase in L leads to an increase in normal force N. In Figure 4 F_{tan} (theoretical) is the contact patch friction force theoretically required to maintain the equilibrium vector diagram of Figure 2, and μN is the saturation limit for friction forces so that $F_{tan} = \mu \cdot N$ is the maximum available force. Using equation (2), the region of smaller L/V ($0<L/V<0.66$) in Figure 4 would require a theoretical value of F_{tan} (theoretical) $\geq \mu \cdot N$ for equilibrium. However, the maximum value that Ftan can attain is the saturation value $\mu \cdot N$. Therefore, in this region for L/V less than 0.66, the actual tangential force is saturated at the value $\mu \cdot N$ which is below F_{tan} (theoretical), and consequently sliding on the flange contact point occurs with the flange contact point moving downwards relative to the rail. Both Figure 4 and 5a clearly show the effects of differing values of F_{tan} (theoretical)

and $\mu \cdot N$. In this region of smaller L/V, the wheel contacts the rail at two points – the tread and the flange (Figure 3). As L increases to 0.66, N and correspondingly $\mu \cdot N$ increase while F_{tan} (theoretical) decreases until equality is reached at F_{tan} equal to $\mu \cdot N$, which is precisely when Nadal's L/V Limit is reached for the start of wheel climb. This is exactly the calculation from Nadal's formula, equation (3) which predicts the onset of climb at L/V=0.66 for the parameters of this case. For L/V ≥ 0.66 in Figure 4, where F_{tan} (theoretical) ≤ $\mu \cdot N$, flange sliding has stopped and flange climb (and hence wheel climb) is occurring with rolling up the rail. It is important to note that in this region for L/V > 0.66 the resultant wheel/rail load R (as shown in Figure 5b) increases along with changes in its orientation to produce an increase in N (and also $\mu \cdot N$) along with a decrease in F_{tan} (theoretical) so that wheel/rail surface conditions are sufficient for wheel climb to develop. In other words, as long as $\mu \cdot N \geq F_{tan}$ (theoretical) the wheel can climb (roll) up the rail

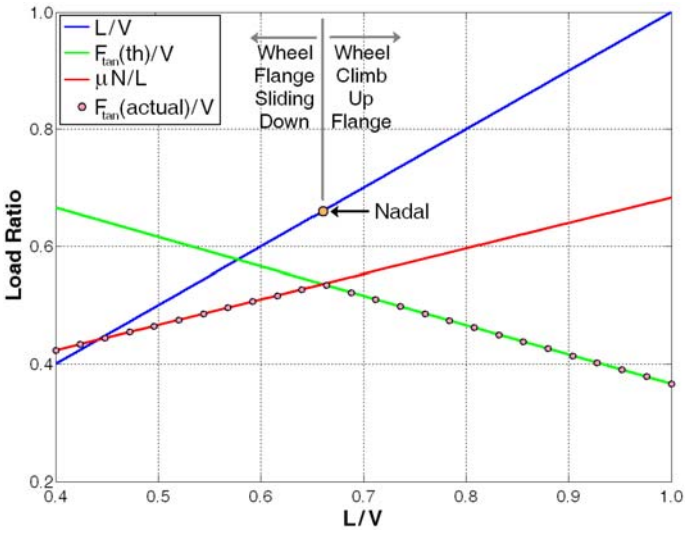

Figure 4 Relation between L/V and flange and flange friction force (μ = 0.5 and V=12,500 pounds)

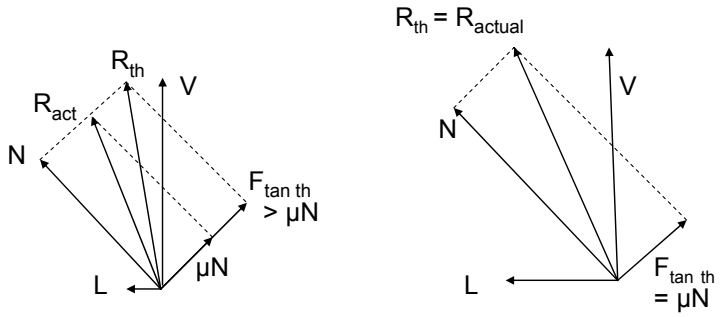

(a) **(b)**

(L/V<0.66) Flange Sliding **(L/V=0.66) Wheel Climb on Flange**

Figure 5 Wheel/Rail forces and saturation

on its flange. This explains why the value of contact friction force is not the only criterion for wheel climb. Depending on the value of lateral force L, the relationship of F_{tan} to both $\mu \cdot N$ and F_{tan} (theoretical) can predict the onset of wheel climb. Also note that tread contact ceases with wheel climb producing a single point of W/R contact. It is important to note that the direction of the actual tangential flange force F_{tan} remains the same whether the wheel is climbing up or the flange contact point is sliding down relative to the rail.

As lateral force L varies, wheel climb begins for $\mu \cdot N = F_{tan}$ (theoretical), while an equilibrium calculation of $\mu \cdot N < F_{tan}$ (theoretical) produces flange sliding. It is useful to further investigate the wheel forces and their resultant associated with these conditions, as shown in Figure 5. In Figure 5a two different resultant wheel forces are shown. One resultant R_{th} is based on L, V components in track coordinates while the other R_{act} is based on the saturated contact friction force which produces $\mu \cdot N$, N in contact coordinates. The actual resultant R_{act} is smaller and of different orientation from the theoretical resultant R_{th} required for a possible wheel climb condition. Actually, we are in the range of F_{tan} (theoretical) ≥ $\mu \cdot N$ so R_{th} cannot exist and the wheel will continue to experience a downward sliding on its flange as it moves forward along the rail. In Fig. 5b the resultant formed by both L, V and $\mu \cdot N$, N are identical with the same contact friction force. Since R_{th} and R_{act} are equivalent to the F_{tan} (theoretical) = $\mu \cdot N$ condition discussed in Figure 4, this force scenario supports a wheel climb condition. A good analogy for these force conditions are the conditions for the slipping (spinning) and/or rolling of a disk in rigid body mechanics. Relations between the disk forces and geometry, subject to a friction saturation constraint, determine the dynamic motion of the disk as discussed in the next section.

DISK SLIPPING (SPINNING) AND ROLLING ANALOGY

A good analogy to the railroad wheel model is a wheel with a torque T applied to its axle (Figure 6). A typical practical case is the tire of a car on an icy patch. Assume that the wheel is spinning due to the low friction at the ground interface. There is a theoretical friction force $F_{th} = T/R$ that must be generated in order for the wheel to stop spinning and to roll forward. However, the actual friction force generated, F_{act} , is limited by the Coulomb saturation value $\mu \cdot N$ where μ is the coefficient of friction and N is the normal force generated at the ground contact point. There are two obvious ways to increase F_{act} - increase the coefficient of friction (e.g., put sand at the contact point), or increase the normal force (e.g., someone sitting on the car fender). This relation between F_{act} and F_{th}, and the parameters μ and N, is also shown in Figure 7 for two different coefficients of friction μ_1 and μ_2. The actual friction force F_{act} is shown increasing with N, for any value of μ to a maximum value of $\mu \cdot N$. When F_{act} reaches F_{th} the wheel will "catch", the

spinning will stop, and the wheel will roll forward without spinning. Note that when $F_{act} = F_{th}$ a free body diagram shows that sum of the moments on the wheel is zero. Based on this analysis it follows that the wheel will roll without spinning as long as the actual contact friction force F_{act} is equal to or greater than the theoretical friction force F_{th} (= T/R). Since the friction force varies with N, the region above F_{th} is denoted as "available friction force" F_{avail}.

These disk friction force concepts are similar to the actual and theoretical friction forces, generated in the flange contact plane for a railroad wheel in flange contact. As discussed previously and depicted in Figure 5, in order for the (F_{tan}, N) vector resultant to be equal to the (L, V) vector resultant R, it is necessary that F_{tan} (actual) = F_{tan} (theoretical). The L/V value associated with this friction equality is precisely the Nadal limit (Figure 5). Also note that similar to the disk analogy, as long as $\mu N \geq F_{tan}$ (theoretical), than the railroad wheel can climb on its flange. Also for consistency in the analogy between the railroad wheel and this rolling disk, the line denoted by $\mu \cdot N/V$ in Figure 4 (for L/V > 0.66) can be denoted as the available dimensionless friction force.

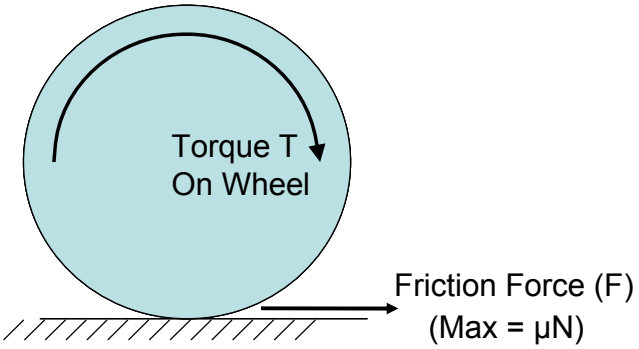

Figure 6 Applied torque on disk resisted by friction force

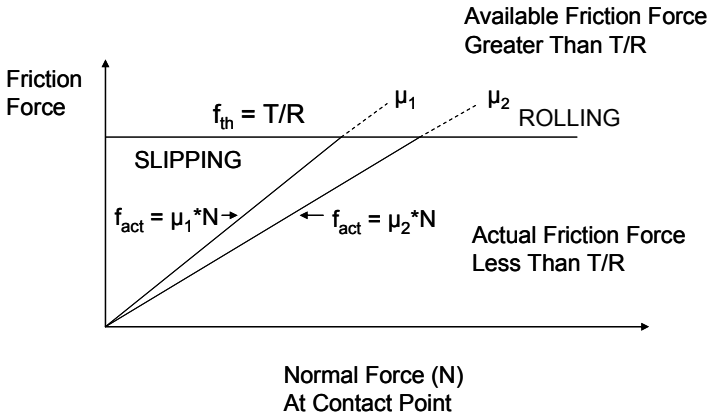

Figure 7 Force on disk versus normal force at Contact point

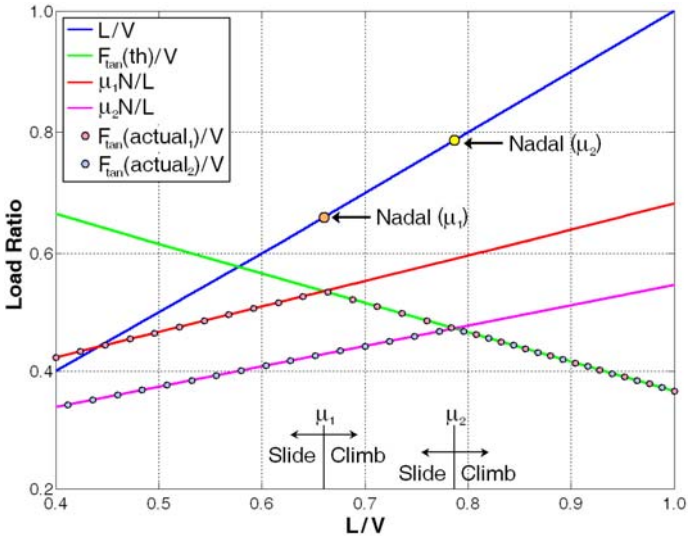

Figure 8 Coefficient of friction variation and Nadal Limit (μ_1=0.5, μ_2=0.4, δ=60, V=12,500 pounds)

FRICTION SATURATION AND NADAL LIMIT

The Nadal Limit increases as friction coefficient μ decreases. This result also can be obtained from equation (3) relating L/V to tan δ and μ. Another interpretation can be found by reconstructing Figure 4 for two different values of μ. This is shown in Figure 8 for values of μ_1 = 0.5 and μ_2 = 0.4. Following the same reasoning as in Figure 4, when going from smaller to larger lateral force, wheel sliding on the flange occurs until the actual friction force $\mu \cdot N$ increases in value to the theoretical friction force. When this friction equality occurs the Nadal L/V limit is reached and wheel climb commences. As shown in Figure 8 the line representing the larger friction force $0.5 \cdot N/V$ intersects the theoretical friction force at the lower value of L. For μ_1 = 0.5 climb starts at L/V = 0.66 while for the lower friction coefficient μ_2 = 0.4 climb starts at L/V = 0.79.

EFFECT OF LONGITUDINAL CONTACT FORCE

For rigid axle wheelsets and for certain operating conditions there can be longitudinal friction forces generated on the wheel which have an important effect on the prediction of wheel climb. The Nadal limit is obtained from equation (2) as a minimum L/V associated with the maximum $F_{tan} = \mu \cdot N$ in the lateral plane. However, if F_{long} effects are included and a resultant friction force is constructed from both F_{long} and F_{tan}, than the critical F_{tan} is reduced which produces a larger critical L/V, i.e. a less conservative value than the Nadal limit of equation (3). Consider Figure 9 which includes a longitudinal creep force F_{long}, that affects the orientation of the resultant by the angle β. If it is assumed that saturation occurs when the *resultant* reaches $\mu \cdot N$, than the L/V for the onset of wheel climb

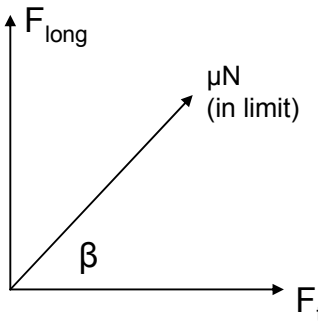

Figure 9 Resultant force on wheel Including effect of longitudinal Force

that is obtained from equation (3) by replacing μ by μ·cosβ (i.e. $F_{tang} = \mu \cdot N \cdot \cos\beta$), leads to a generalized L/V expression of:

$$\text{Generalized L/V} = (\tan\delta - \mu \cdot \cos\beta)/(1 + \mu \cdot \cos\beta \cdot \tan\delta) \quad (4)$$

One interpretation of equation (4) is that it is equivalent to using the Nadal Limit of equation (3) with a reduced value of friction coefficient equal to μ·cosβ. Note that for the angle β = 0, the resultant is oriented in the lateral plane and the generalized L/V expression is equal to the Nadal Limit of equation (3).

The generalized L/V expression corresponding to β = 90, 60, 30, 0 degrees are shown in Figure 10 as a function of friction coefficient μ (with δ =60). These L/V results are less conservative than the Nadal Limit (β = 0) since for a given value of friction coefficient μ, the Generalized L/V > Nadal L/V. For example, for μ = 0.5 and β = 30 degrees, the Generalized L/V = 0.74 while Nadal L/V = 0.66, for a 12.4% increase in L/V before the onset of wheel climb is predicted.

It is useful to calculate a margin of error for L/V defined as (Generalized L/V)/(Nadal L/V). This margin of error, based on the resultant wheel force (for β = 90, 60, 30, 0) is shown in Figure 11 as a function of friction coefficient μ. This margin of error increases with both μ and deviation of the resultant from the lateral orientation (i.e., β). As an example, for β = 30 degrees (i.e. $F_{tan} = 0.866 \cdot \mu \cdot N$), the margin of error ranges from 12% to 29% as μ varies from 0.5 to 1. Therefore, basing wheel climb on the resultant force rather than just the tangential friction force F_{tan} can lead to a prediction of the onset of wheel climb that is higher than the Nadal prediction, and hence is a less conservative indicator.

RELATIONSHIP OF ANGLE OF ATTACK TO L/V AND NADAL LIMIT

The proceeding discussion involving lateral and longitudinal creep forces, saturation, and onset of wheel climb can also be related to wheelset angle of attack. It has been verified in field

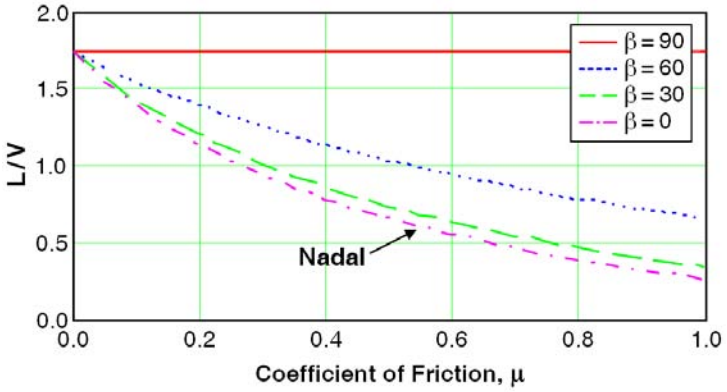

Figure 10 L/V vs. friction coefficient μ, based on resultant wheel force for Ftan = μ·N cosβ (β = 90, 60, 30, 0 degrees)

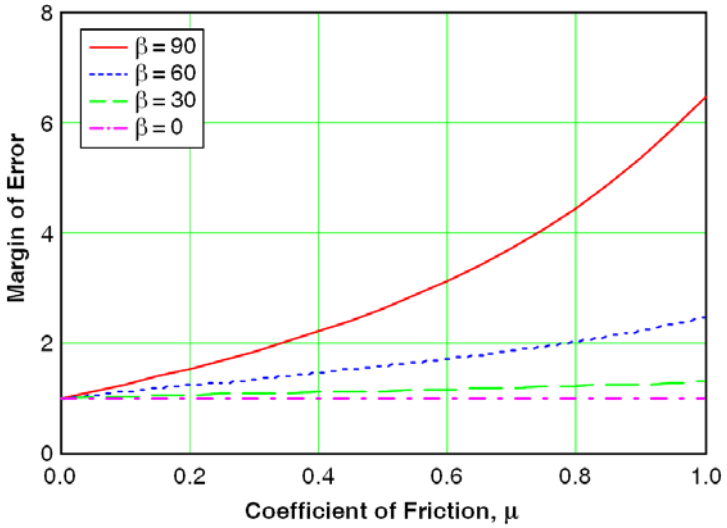

Figure 11 Margin of error (ratio of Generalized L/V to Nadal L/V) as a function of friction coefficient μ

tests and shown in References [2]-[6] that the Nadal limit, equation (3), is a good predictor of the onset of wheel climb when the wheelset has a large angle of attack orientation and the longitudinal creep force is small. However, as the angle of attack decreases, the Nadal limit becomes more conservative, i.e. it predicts a smaller L/V ratio than is actually required for wheel climb. An interpretation [3] of this important angle of attack effect can be made by relating lateral contact (creep) force F_{tan} to the lateral creep velocity v_{creep} (neglecting the effect of spin creep):

$$v_{creep} = (\psi - \dot{y}/V)/\cos\delta \quad (5)$$

where ψ is the axle yaw angle, $\dot{y}$ is lateral velocity, V is the forward velocity of the wheelset and δ is the flange angle. The

term ($\psi - \dot{y}/V$) is referred to as effective angle of attack, which for steady state conditions simply reduces to yaw angle ψ. Rewriting, for convenience in interpretation, equation (2) which relates forces in track and contact coordinates gives:

$$L/V=(\tan\delta-F_{tan}/N)/(1+(F_{tan}/N)\cdot\tan\delta) \qquad (2)$$

An understanding of the importance and origin of the longitudinal creep force is important since its value on the low wheel and flanging wheel are generally the same. When the angle of attack is large, F_{tan} is large and can reach saturation so that (F_{tan}/N) can be replaced by μ which transforms this L/V relationship of equation (2) to the Nadal L/V of equation (3). Of course, in this range of large AOA, F_{long} is smaller since it is the resultant of (F_{tan} , F_{long}) that reaches μN. Alternatively, when the angle of attack is reduced the lateral creep and hence F_{tan} is reduced and F_{long} is increased when the resultant saturates. Substituting this reduced value of F_{tan} /N into equation (2) leads to a L/V ratio higher than the Nadal L/V of equation (3) because in the Nadal Limit F_{tan} /N has been replaced by μ. Thus for this smaller angle of attack case, the Nadal limit is conservative since it predicts a smaller L/V (perhaps significantly smaller) for the prediction of onset of wheel climb. Finally, although not addressed in this paper, it should be noted that if the AOA becomes negative both the creep and sliding force act against wheel climb, and subsequently a much larger lateral force is required on the flanging wheel in order for wheel climb to occur.

CONCLUSIONS

The conditions required for flange climb derailment are investigated in terms of the wheel-rail forces developed by an axle in steady state motion along a railroad track. One of the first studies of this phenomenon was done by Nadal who related flanging wheel force in track coordinates to equivalent forces in contact coordinates. This produces a relationship between (L, V) the lateral and vertical wheel loads in track coordinates, and the forces in the flange contact plane (F_{tan}, N) the tangential friction force due to creep and the normal force, respectively. This relationship leads to the Nadal Limit for the prediction of the onset of wheel climb which is accurate for high angle of attack conditions.

In this paper a detailed study is made of the variation of F_{tan} and N, both of which vary as a function of lateral load L. The region where the flange contact point slides down the rail with a saturated value of F_{tan} is shown as a function of lateral load, as the wheelset moves along the rail. The value of L at which F_{tan} is about to drop *below* its saturated value is the point at which the flange contact condition will *change from sliding down the rail to a climbing* (rolling) upward on the rail as the wheelset travels along the rail. This point for the onset of wheel climb is shown to be precisely the Nadal Limit, and L/V can then be written in terms of the friction coefficient μ between the flanging wheel and the rail, and also δ the flange contact angle. These results also explain why, depending on the value of L, for the same value of F_{tan} the wheel may climb up or it may experience sliding down on its flange. This paper also introduces an alternative explanation for the wheelset climb prediction based on a comparison of the flanging wheel force resultant in track coordinates with the contact plane force resultant.

A useful analogy for understanding these concepts are the conditions for the sliding (spinning) and/or rolling of a disk in rigid body mechanics. An example is shown relating disk forces and disk geometry (subject to a friction constraint) to the ensuing dynamic rolling motion of the disk. Two further effects are studied for their impact on wheel climb conditions – effect of longitudinal creep and also the effect of wheelset angle of attack. The resultant friction force in the contact plane includes a component in the longitudinal direction due to longitudinal creep. Since friction saturation implies resultant saturation $\mu \cdot N$, than a reduced F_{tan} associated with the component of the saturated resultant is the proper force to use in predicting the onset of wheel climb. This produces a generalized L/V expression which is larger (and thus less conservative) than the Nadal Limit in predicting wheel climb. The second effect, namely angle of attack (AOA), is important because F_{tan} is proportional to angle of attack and than amplified by the flange angle. A larger AOA is consistent with Nadal's original assumptions while for a smaller AOA the Nadal limit is conservative, because it predicts a smaller critical L/V (perhaps significantly smaller) for the prediction of the onset of wheel climb.

ACKNOWLEDGEMENTS

This work was sponsored by the FRA Office of Research and Development, Track Research Program.

REFERENCES

(1) Nadal, M.J. 1896 "Theorie de la Stabilite des locomotives, Part II:mouvement de lacet", Annales des Mines, 10, 232.
(2) Gilchrist, A.O., and Brickle, B.V., 1976 " A Re-Examination of the Proneness to Derailment of a Railway Wheelset", Journal of Mechanical Engineering Science, Vol. 18, No. 3, pp 134-141.
(3) Weinstock, H., 1984, "Wheel Climb Derailment Criteria for Evaluation of Rail Vehicle Safety", ASME Paper 84-WA/RT-1. Presented at 1984 Winter annual meeting, Phoenix, AZ.
(4) Shust, W.C., and Elkins, J.A., 1997, "Wheel Forces During Flange Climb, Part I – Track Loading Vehicle Tests", Proceedings – IEEE/ASME Joint Railroad Conference, Boston, MA.

(5) Elkins, J.A., and Shust, W.C., 1997, “Wheel Forces During Flange Climb, Part II– Nucars Simulations”, Proceedings – IEEE/ASME Joint Railroad Conference, Boston, MA.
(6) Blader, F. B., 1989, “Assessing Proximity to Derailment from Wheel/Rail Forces: A Review of the State of the Art”, presented at 1989 ASME Winter Annual Meeting, San Francisco, CA.
(7) Blader, F. B., 1990 , A Review of Literature and methodologies in the Study of Derailment Caused by Excessive Forces at the Wheel/Rail Interface”, Association of American railroads, Report R-717.
(8) US Department of Transportation, FRA, “49 CFR Parts 213 and 238 – Vehicle/Track Interaction Safety Standards; High-Speed and High Cant Deficiency Operations; Proposed Rule,” Federal Register May 10, 2010.